
MAIN STATISTICAL PROPERTIES OF HECTOMETRIC CONTINUUM RADIATION IN NEAR-EARTH SPACE

D.A. Dorofeev

*Higher School of Economics,
Moscow, Russia, dadorofeev_1@edu.hse.ru
Space Research Institute RAS,
Moscow, Russia*

A.A. Chernyshov 

*Space Research Institute RAS,
Moscow, Russia, achernyshov@cosmos.ru*

D.V. Chugunin 

*Space Research Institute RAS,
Moscow, Russia, dimokch@iki.rssi.ru*

M.M. Mogilevsky

*Space Research Institute RAS,
Moscow, Russia, mogilevsky2012@gmail.com*

Abstract. In this work, we have studied the recently discovered hectometric continuum radiation in near-Earth plasma. We have carried out a detailed statistical analysis of the occurrence of a hectometric continuum near Earth at distances $1.1\text{--}2 R_e$, where R_e is the Earth radius, for a two-year period, using data from the ERG (Arase) satellite. We have established that the generation of the hectometric radiation depends on the local magnetic time. The continuum radiation of this type is shown to occur mainly at night and in the morning. We have also studied the dependence of the occurrence of hectometric radiation on geomagnetic activity and have

demonstrated that there is no direct dependence of the occurrence of hectometric radiation on geomagnetic disturbances. Moreover, the statistical analysis made it possible to localize sources of radio emission of this type in near-Earth space and to show that the source(s) of generation of the hectometric continuum radiation is located at low latitudes.

Keywords: radio emission, hectometric continuum radiation, magnetosphere, satellite measurements.

INTRODUCTION

There are three natural electromagnetic emissions that are generated in near-Earth space at frequencies above the electron gyrofrequencies and can only be studied with spacecraft: the auroral kilometric radiation (AKR), the non-thermal continuum radiation, and the recently discovered hectometric radiation.

AKR is a high-power non-thermal radio emission in the frequency range 30–800 kHz, which is generated near the local cyclotron frequency of electrons in the auroral region of Earth's magnetosphere. AKR was first detected by the Electron-2 satellite in 1965 [Benediktov et al., 1965]. Numerous measurements with high-apogee satellites have determined the main parameters of AKR, its properties, and the conditions under which this radiation is generated [Gurnett, 1974; Treumann, 2006; Louarn, Le Quéau, 1996; Benson, Calvert, 1979; Hanasz et al., 2001; Chugunin et al., 2020; Kolpak et al., 2021; Chernyshov et al., 2022]. For more than a decade, various theories of the generation of such radiation had been put forward until the mechanism of cyclotron maser instability was proposed to explain the occurrence of AKR [Wu, Lee, 1979]. This mechanism is generally accepted at present. The instability develops in the auroral magnetosphere in regions with a low plasma density (caverns), where the electron plasma frequency is lower than the local cyclotron frequency of electrons [Wu, Lee, 1979]. The AKR-type radiation is observed in magnetospheres of other planets having strong self-magnetic fields, such as Jupiter, Uranus, and Saturn [Zarka, 1998].

The non-thermal continuum is also a fundamental electromagnetic emission in planetary magnetospheres

and is detected in a very wide frequency range — from 5 kHz [Gurnett, 1975; Brown, 1973] to 800 kHz [Hashimoto et al., 1999; Kuril'chik et al., 1992]. Although the term "non-thermal continuum" implies continuous radiation, in fact it refers only to its lowest frequency range. The non-thermal continuum actually consists of discrete radiation bands, and in some cases it turns out to be connected with strong narrow-band electrostatic emission at the plasmopause in low latitudes [Kurth, 1982]. The non-thermal continuum is often divided into radiation trapped in Earth's magnetosphere and radiation escaping from the magnetosphere [Green et al., 2004]. Of particular note is the non-thermal continuum component called kilometric continuum. The kilometric continuum radiation is generated only in a high-frequency part of the spectrum (above 100 kHz) by the same mechanism as the low-frequency non-thermal continuum radiation [Green et al., 2004]. The question about the physical mechanism (or mechanisms) of generation of continuum radiation has not been answered in full yet.

Moreover, in Earth's magnetosphere there is a higher-frequency radiation, 600–1700 kHz, whose spectrum is a set of individual frequencies (a linear spectrum). This radiation was termed "hectometric continuum radiation" [Mogilevsky et al., 2021; Kuril'chik, 2007; Hashimoto et al., 2018]. From ERG (Arase) measurements of the electromagnetic field electric component in the frequency range 2 kHz – 10 MHz, the generation regions of the kilometric continuum radiation and the recently discovered hectometric continuum radiation have recently been identified [Mogilevsky et al., 2021]. Both radiations have a linear spectrum. The kilometric continuum is shown to occur mainly in the dayside magne-

tosphere, its source is located near the plane of the geomagnetic equator, and the dimensions of the source do not exceed $\pm(0.1\div 0.3) R_E$ across this plane, where R_E is the Earth radius. The hectometric radiation that is generally observed in the nightside magnetosphere most likely has two generation regions: one is located near the plasmasphere at distances to $3 R_E$; the second, near Earth at distances from $1.1 R_E$ to $2 R_E$. The spectral and frequency characteristics of the hectometric radiation from both sources were noted to be almost identical; the only difference is the location of the source. Since earlier the hectometric radiation has been investigated using either case study [Mogilevsky et al., 2021] or extremely limited statistics whose results are significantly affected by the satellite orbit [Hashimoto et al., 2018], it is necessary to perform a detailed statistical analysis to determine the main properties and characteristics of radiation of this type.

The mechanism of excitation of radio emission of this type in near-Earth plasma is still in question. The physical mechanism of generation of non-thermal kilometric continuum radiation is still unclear despite the longer history of its study compared to the hectometric radiation. The most probable are nonlinear models of three-wave interaction: coalescence of an electrostatic Bernstein wave with a low-frequency one and their subsequent transformation into an electromagnetic mode [Melrose, 1981], or disintegration of the electrostatic wave into a low-frequency one and electromagnetic X- or O-mode [Ronmark, 1985]. Alternative mechanisms are associated with the linear transformation of the Z-mode of radiation into an ordinary wave near the plasma frequency [Jones, 1980] or with the assumption that the ordinary mode can be excited by electrostatic fluctuations [Okuda et al., 1982]. It is possible that the previously proposed mechanisms for generating the non-thermal continuum can also be applied to hectometric radiation. This issue requires a follow-up study. In addition, there may be a mechanism of double plasma resonance [Zheleznyakov et al., 2016] when either upper or lower hybrid resonance frequencies coincide with one of the gyrofrequency harmonics resulting in excitation of plasma waves that are transformed into intense electromagnetic radiation through the mechanism of three-wave interaction.

Since the hectometric radiation has been discovered quite recently, there are many open questions concerning, for example, its relationship with geomagnetic and solar activity. This issue has not been investigated at all so far. There are different points of view on such a relationship for the kilometric continuum. Hashimoto et al. [2005] have observed that the kilometric continuum occurs more often during solar minimum than during solar maximum. Yet, Kuril'chik et al. [2004] have found only a small difference in the rate of recurrence with solar cycle and have recorded more cases of kilometric continuum generation during solar maximum than during solar minimum. The kilometric continuum was observed during periods of both low and high geomagnetic activity, with no significant correlation of wave intensity with the K_p index [Green et al., 2004]. Nonetheless,

the maximum observed radiation frequency of the kilometric continuum statistically tends to increase with an increase in the K_p index; the effect is more pronounced near solar maximum, but is also detected near solar minimum. There is strong evidence that the source region of the kilometric continuum is close to the equatorial plasmapause during periods when the position of the plasmapause is significantly shifted to Earth [Green et al., 2002]. At the same time, AKR increases during magnetic disturbances and correlates well with the high-latitude geomagnetic index AE [Voots et al., 1977], which measures the current flowing in the ionosphere. In other words, AKR is recorded only during geomagnetic disturbances. In addition, there is a clear seasonal dependence of AKR intensity [Kasaba et al., 1997] because the radiation is more active at high frequencies in the winter polar region. Morooka, Mukai [2003] have found a seasonal dependence of the height profile of acceleration region and have suggested that a change in the height of the longitudinal particle acceleration region depends on the density of the background plasma originating from the ionosphere. Since ionospheric plasma properties vary depending on season, the average position of the radiation region also differs in height in winter and summer [Mogilevsky et al., 2005]. For the hectometric radiation, the seasonal dependence is also an open question.

In this paper, for the first time we have examined the main statistical properties of the hectometric continuum at distances to $2.1 R_E$ inclusive for two full years, using data from the ERG (Arase) satellite. It has previously been shown [Mogilevsky et al., 2021] that sources of the hectometric continuum radiation are observed both near Earth at distances of $(1.1\div 2)R_E$ (let us call the hectometric radiation of this type "type A radiation") and in the plasmasphere at distances of $(4\div 6)R_E$ (type B radiation). Sources of the non-thermal kilometric continuum, which has previously been studied with various spacecraft, are also assumed to be located near the plasmasphere [Green et al., 2002, 2004; Carpenter et al., 2000]. We have chosen the type A hectometric continuum for detailed analysis in order to identify properties of the recently discovered continuum, which in the future should help in constructing a physical mechanism for generating hectometric radiation. Over the period from 2018 to 2019, 279 cases of hectometric continuum observation were found in ERG (Arase) satellite data, which allows us to accurately localize the sources of the hectometric radiation, as well as to identify the dependences of hectometric continuum generation on local magnetic time (MLT) and on season. In addition, such extensive statistics makes it possible to figure out whether there is a relationship between the occurrence of hectometric radiation in Earth's magnetosphere and geomagnetic activity.

STATISTICAL ANALYSIS

The Japanese satellite ERG — Exploration of energization and Radiation in Geospace (renamed Arase after entering orbit) [Miyoshi et al., 2018a, b] was launched on December 20, 2016. Orbit parameters: ap-

ogee is ~ 32000 km, perigee is ~ 400 km, inclination is 31° . The satellite's period is ~ 570 min. The ERG (Arase) satellite is oriented toward the Sun and is stabilized by rotation around this direction with a period of 8 s. More detailed information about the ERG (Arase) satellite's orbit and its changes is available in [Miyoshi et al., 2018a] and in Figures therein. The magnetic local time of the apogee was initially nine, and then MLT of the apogee shifted from dawn to dusk during the night. The apogee line shifts in local time at a rate of $\sim 260^\circ$ per year clockwise. It is, therefore, necessary to have extensive statistics to minimize the influence of the ERG (Arase) satellite's orbit on the results.

The scientific equipment of the satellite is designed primarily to examine physical processes in the Earth radiation belts, but the wide measuring capabilities of the complex of scientific instruments also allow for the study of radio emission of various types on our planet. To study the hectometric continuum radiation, we have used measurements of the electric field component made during the PWE/HFA experiment [Kasahara et al., 2018; Kumamoto et al., 2018].

The top panel of Figure 1 exemplifies a type A hectometric continuum radiation recorded by the ERG (Arase) satellite on August 16, 2019. The satellite is in the Northern Hemisphere all the time of observation — the z coordinate in the solar magnetic coordinate system (z_{sm}) varies from $1.0 R_E$ to $\sim 2.7 R_E$; and the McIlvaine parameter L , from ~ 2.6 to ~ 7.0 . MLT varies from ~ 00 to ~ 05 , which corresponds to the night/morning side of the magnetosphere. The linear spectrum in the 850–1700 kHz frequency range at a distance of order of $R=1.8 R_E$ is a hectometric continuum radiation that lasts for ~ 3 hrs ($\sim 09:02$ – $11:02$ UT) and ends at $R=5.0 R_E$. The radiation reaches a maximum intensity of 10^{-7} mV/m Hz approximately 10 min after the start of observation at 09:12 UT, which corresponds to $R=2.2 R_E$. It is worth noting that between 09:02 and 09:50 UT there is a type A radi-

ation whose intensity begins to fall after a maximum at 09:12 UT. Then, around 10:00 UT, radiation must have been recorded from another source, located at a greater distance from Earth ($\sim 3.7 R_E$) — near the plasmopause, which indicates the generation of a type B hectometric continuum. Interestingly, in the top panel of Figure 1, starting at 09:00 UT in frequencies below 1000 kHz there is an auroral kilometric radiation (AKR) that also occurs during the event considered, with the AKR power being significantly higher than the hectometric radiation power. To the left of the hectometric continuum and below it, there is also a region of radiation at the upper hybrid resonance frequency.

The bottom panel of Figure 1 illustrates a similar, but shorter-period hectometric continuum radiation recorded on May 11, 2019. The observed frequency range for this event is somewhat narrower: ~ 1000 – 1650 kHz. The hectometric continuum radiation begins to be recorded at $R=1.3 R_E$, lasts for 26 min ($\sim 09:45$ – $10:11$ UT), and ends at $R=2.2 R_E$. MLT varies from ~ 3.5 to ~ 7 , which also corresponds to the night/morning side. In the event at hand, the satellite crosses the plane of the geomagnetic equator from the Southern Hemisphere to the Northern Hemisphere — z_{sm} varies from -0.1 to $0.8 R_E$. The L parameter increases from 1.3 to 2.6. The radiation reaches its maximum intensity ($>10^{-7}$ mV/m Hz) 8 min after the start of observation, at $\sim 09:53$ UT, at $R=1.5 R_E$. As in the previous case, there is a region of increased intensity at the upper hybrid resonance frequency on the spectrum to the left of the hectometric region and below it.

Next, we examined the relationship between the occurrence of the hectometric continuum radiation and geomagnetic activity by analyzing the geomagnetic index Dst . We used estimated Dst for the moments of maximum intensity of the hectometric radiation and constructed corresponding histograms (Figure 2). The top histogram displays the distribution of hectometric radiation observations depending on the Dst index

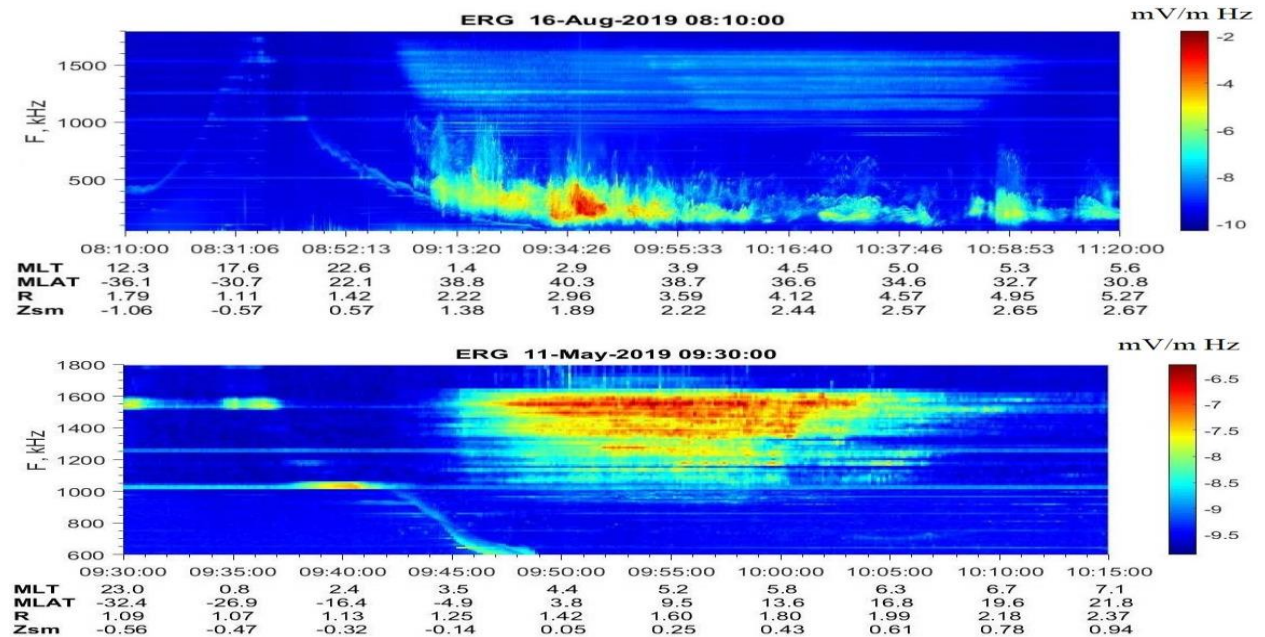


Figure 1. Hectometric continuum radiation on spectrograms of the electric field component for August 16, 2019 in the frequency range 50–1800 kHz (top panel) and for May 11, 2019 in the frequency range 600–1800 kHz (bottom panel)

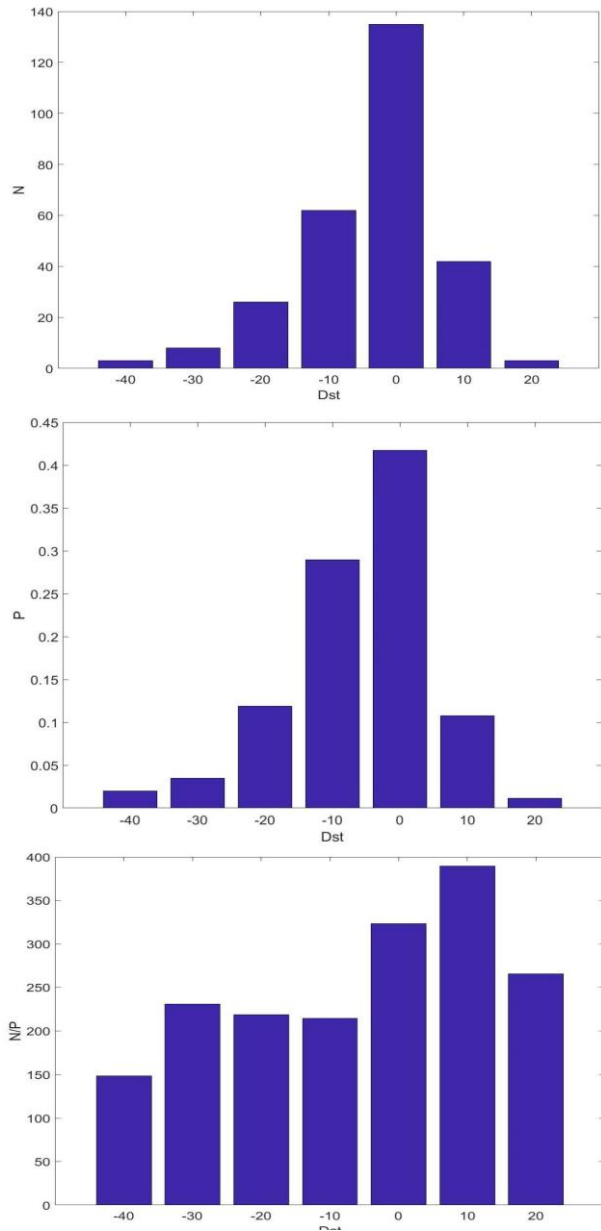


Figure 2. Distribution of cases of hectometric continuum radiation observation over the Dst index (top), the probability of distribution of the Dst index for 2018–2019 (middle), and the number of cases normalized to the probability of distribution of the Dst index for 2018–2019 (bottom)

[World Data Center for Geomagnetism, 2015]. The middle panel demonstrates the probability distribution of Dst values for 2018–2019. This distribution is seen to be similar to the distribution of cases of hectometric continuum detection with the ERG (Arase) satellite in the top panel of Figure 2; therefore, for a more correct analysis we constructed a histogram with a number of cases normalized to the probability of distribution of the Dst values for 2018–2019 (bottom panel). This histogram (bottom panel in Figure 2) suggests that in fact there is no direct relationship between the occurrence of the hectometric continuum and geomagnetic activity.

Statistical analysis has also been carried out for other parameters of the hectometric radiation. Figure 3 presents histograms of the events over months for 2018 and 2019 separately and in total. Comparing histograms for 2018 (top panel) and 2019 (middle panel), we can note the absence of type A events from May to August 2018, yet already in 2019 the hectometric continuum is not observed only in March, and from May to August a sufficient number of events are recorded. Such differences between the observations arise due to the precession of the ERG (Arase) satellite's orbit because in the histogram for the two years the hectometric radiation is observed every month and there are no gaps in the distribution. This proves once again that to draw correct conclusions it is necessary to have large statistics minimizing the impact of the spacecraft orbit.

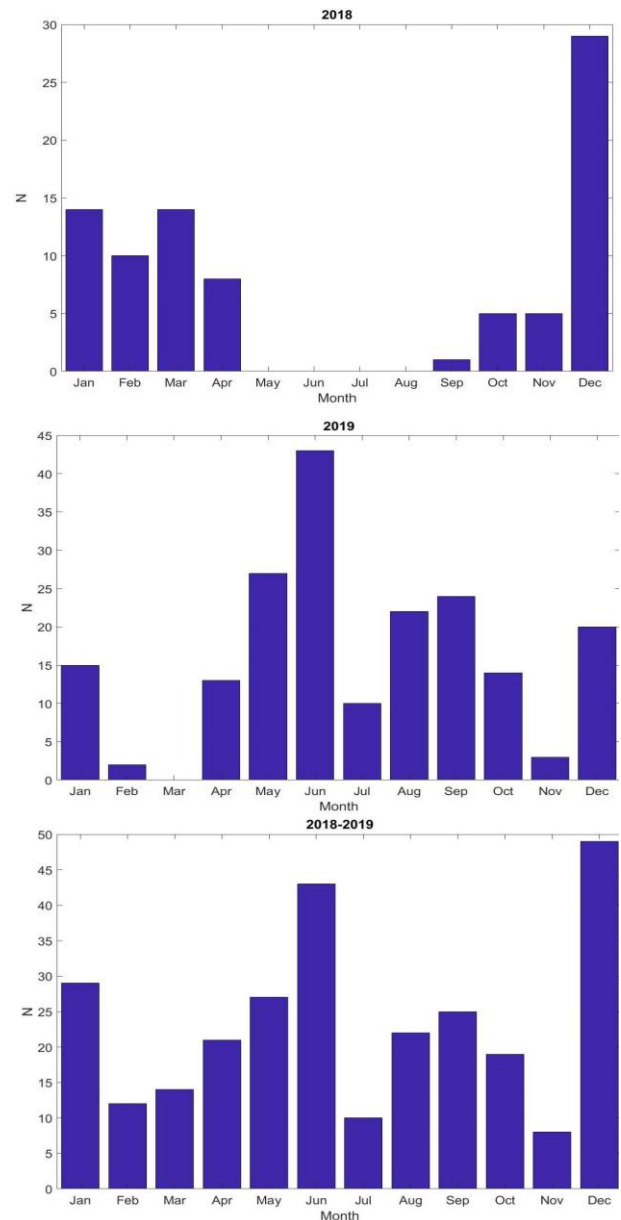


Figure 3. Distribution of cases of hectometric radiation observation over months for 2018 (top), 2019 (middle), and for the two years (bottom)

At the next stage of data analysis, we constructed a two-dimensional histogram of the magnetic latitude (*MLAT*) of the satellite's orbit over months, as well as the satellite's *MLAT* at the time of hectometric continuum radiation observation over months (Figure 4). The former histogram (left panel in Figure 4) shows the apparent dependence caused by the ERG (Arase) satellite's orbit.

A similar dependence can also be seen in the second histogram (right panel in Figure 4). However, in the right panel are well-defined cases in addition to those in the main dependence — the largest number in January and December, which does not agree with the histogram of the satellite's orbit in the left panel. Such cases indicate that physical processes in near-Earth space can influence the results of hectometric radiation observation. Note that unlike the winter period when radiation of this type is mainly recorded near the geomagnetic equator, in other months the hectometric radiation is observed at latitudes to 30° N and S.

We have analyzed the relationship between the occurrence of hectometric continuum and the local magnetic time (MLT). The histogram in Figure 5 shows that

the hectometric radiation occurs mainly at night and in the morning. We have thus confirmed the assumption, made by Mogilevsky et al. [2021], about the relationship between the hectometric continuum generation and the local magnetic time. According to the statistical analysis results, the hectometric radiation is observed from 21 to 08 MLT, hence the generation of this continuum may depend on the illumination of the ionosphere.

Figure 6 presents two-dimensional histograms of the z coordinate in the solar magnetic coordinate system (z_{sm}) over the McIlvaine parameter L and the distance R , which allow us to understand the localization of hectometric continuum sources. As inferred from Figure 6, most observations of the hectometric continuum radiation fall within the range from -0.5 to 0.5 in z_{sm} , from 1 to 1.4 in the L parameter, and from 1.1 to 1.25 in the distance R , thereby indicating that the radiation sources are located at low latitudes. Furthermore, it is noticeable that with increasing distance away from Earth the maximum number of hectometric radiation observations moves away from the equatorial region. In other words, the z -coordinate modulus increases with R .

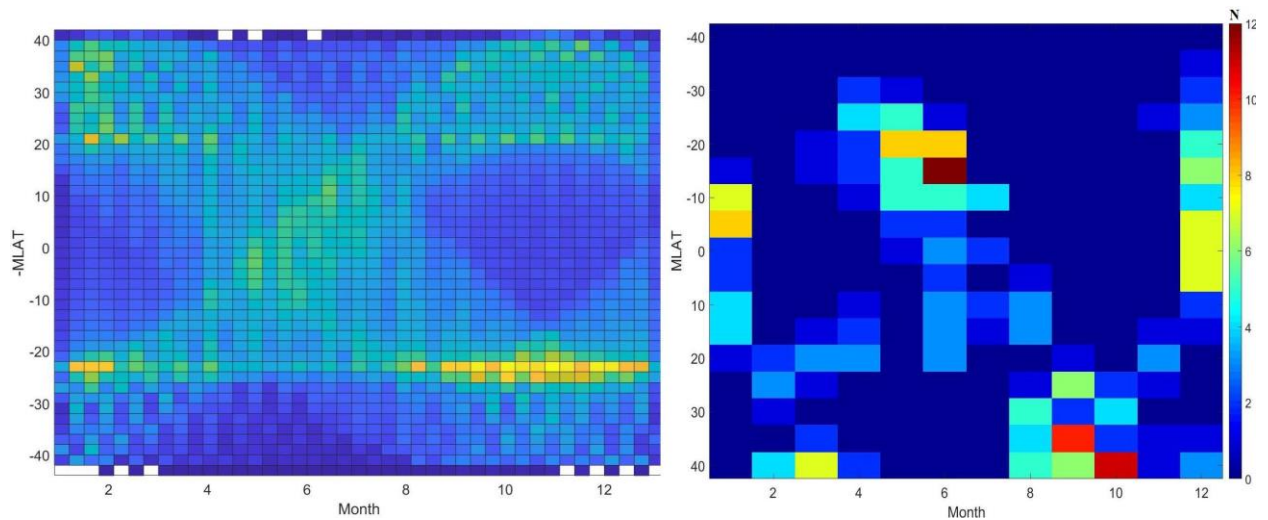


Figure 4. Histograms of the satellite's orbit *MLAT* (left panel) and the satellite's *MLAT* at the beginning of hectometric continuum observation (right panel) over months

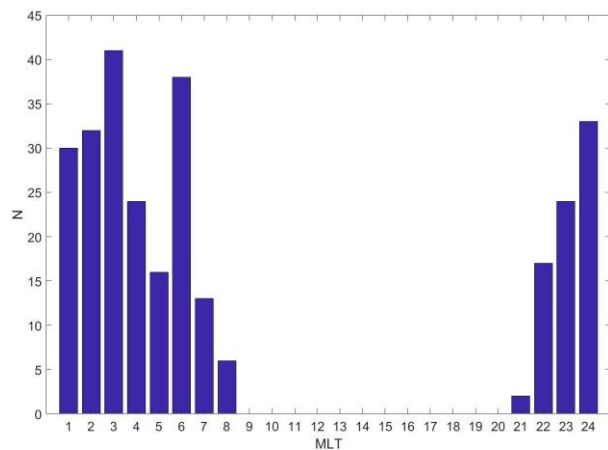


Figure 5. Distribution of cases of hectometric continuum observation by local magnetic time

In addition, we have constructed histograms of cases of hectometric continuum observation over R and L (Figure 7). In the right panel, there is a clear predominance of cases of hectometric continuum observation at short distances of order of $(1.1 \div 1.2)R_E$, the cases of maximum distance were at $\sim 2.1 R_E$. A similar dependence is observed for L : most cases of hectometric radiation detection occur at small L values to 1.5.

SUMMARY AND MAIN CONCLUSIONS

From measurements of the electromagnetic field electric component with the Japanese ERG (Arase) satellite (PWE/HFA experiment), 279 cases of observation of A type hectometric continuum radiation have been found for two full years — 2018 and 2019. We have carried out

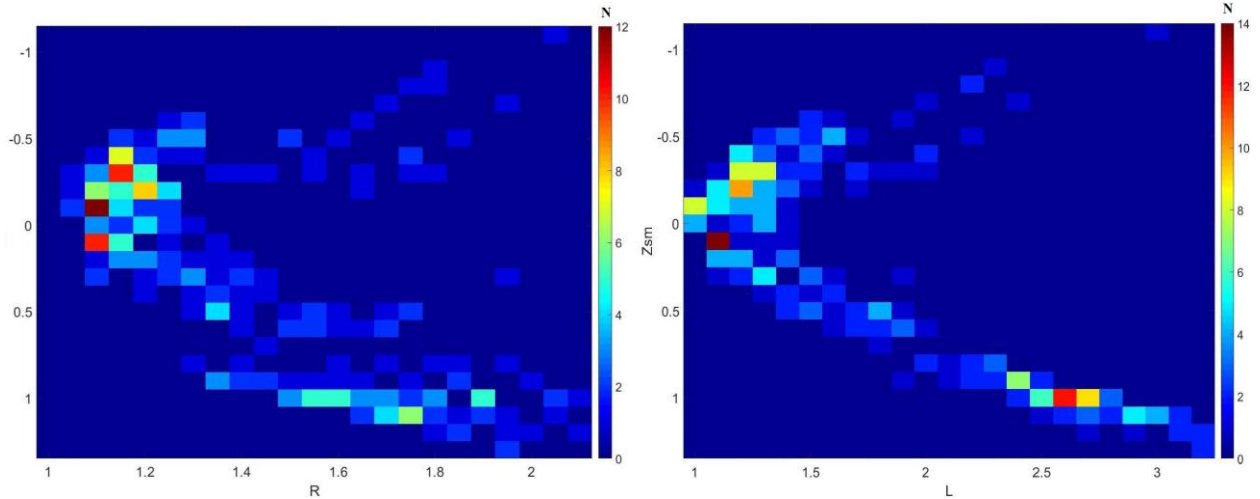


Figure 6. Two-dimensional histograms of the z coordinate (in the solar magnetic coordinate system) over the distance R (left panel) and the McIlvaine parameter L (right panel)

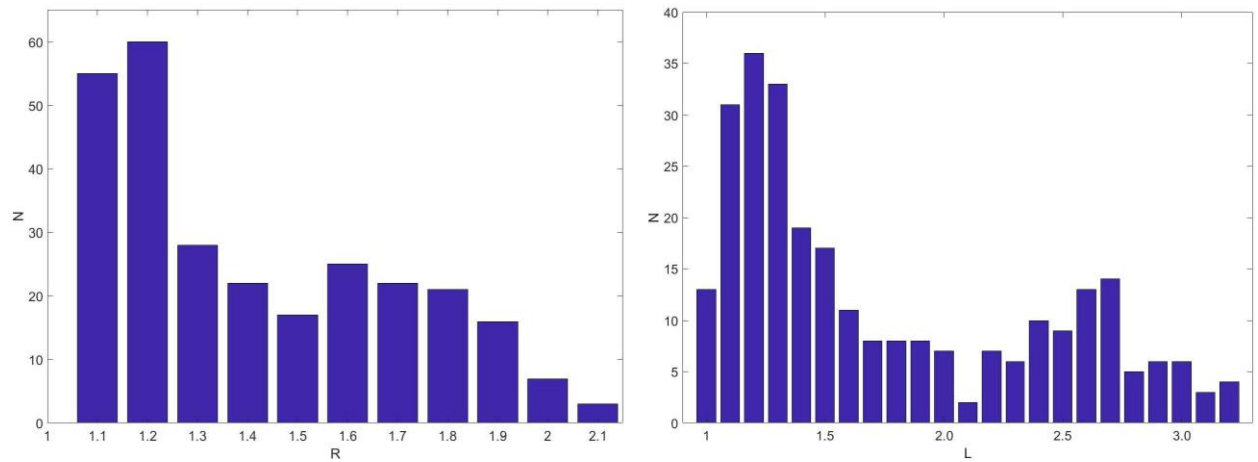


Figure 7. Distributions of cases of hectometric continuum observation over the distance R (left) and the McIlvaine parameter L (right)

a detailed statistical analysis of various parameters of radiation of this type and have identified some of its properties in Earth's magnetosphere.

All cases of the type A hectometric continuum have been recorded at distances to $2.1 R_E$ inclusive. Note that in each case in the spectrograms there is an upper hybrid resonance frequency near which the radiation of this type occurs. In most cases, the radiation begins to be observed at distances of order of $(1.1 \div 1.25)R_E$, which corresponds to the heights of the upper ionosphere and the lower magnetosphere. The hectometric radiation was observed mainly at small values of the McIlvaine parameter L from 1 to 1.4, the distance R varied from 1.1 to 1.25, whereas z_{sm} varied from -0.5 to 0.5 , which may be associated with the satellite's orbit. Thus, the statistical analysis has localized sources of radiation of this type in plasma: the hectometric continuum occurs mainly in the low-latitude region of near-Earth space; therefore, the source (or sources) of this radiation is located at low latitudes.

We have also established that there is no direct relationship between the occurrence of hectometric radiation and geomagnetic disturbances. The absence of an

explicit dependence on the geomagnetic index Dst (a measure of magnetic field variations due to ring currents arising in the magnetosphere during magnetic storms) suggests that the hectometric continuum can be observed both during quiet periods and during strong geomagnetic activity. Earlier in [Hashimoto et al., 2018] based on incomplete statistics for 2017, no significant dependence was found on another geomagnetic index K_p (characterizes the global geomagnetic disturbance in a three-hour time interval), whereas the total number of cases for $K_p \geq 6$ was very small. Note that radiation of other types — AKR and non-thermal continuum — occurs mainly only during geomagnetic disturbances [Kasaba et al., 1998; Kurth et al., 1998]. Since, as is known, AKR and the kilometric continuum are observed in all Solar System planets having magnetic fields [Zarka, 1998; Kurth, 1982], it should be expected that the hectometric radiation is also characteristic of such planets. In this case, the hectometric radiation can be used as an additional indicator of planets (exoplanets) with magnetic fields. The main indicator is AKR whose lifetime depends on geomagnetic activity. According to [Turner et al., 2021], from the processing

results of LOFAR measurements, radio signals that may be cyclotron radiation from an exoplanet with a magnetic field have been detected. In other words, AKR-type radiation from an exoplanet was found, which once again demonstrates the importance of studying properties of radio emission of various ranges.

In this paper, using statistics for full two years, we have confirmed the relationship between generation of the hectometric continuum and local magnetic time, found earlier in [Mogilevsky et al., 2021]. Radiation of this type is observed at night and in the morning. This may be due to a decrease in the electron density in the upper ionosphere and the lower magnetosphere at night.

Note also that the ERG (Arase) satellite's orbit changes have a significant impact on the detection of hectometric continuum. For example, there are fewer cases of type A radiation observation in 2018 than in 2019. The distribution of the hectometric continuum over months for two years does not have such obvious dips and peaks as if we considered separately 2018 or 2019.

Hashimoto et al. [2018] from limited statistics for 2017 have obtained very different results for each month due to peculiarities of the ERG (Arase) satellite's orbit. All this clearly indicates the importance of statistics for as long a period of time as possible in order to minimize the influence of evolution of a spacecraft's orbit when studying and determining hectometric radiation properties.

Similar radiation was observed during the AKR-X experiment with the Interbol-1 satellite at frequencies of 1463 and 1501 kHz [Kuril'chik, 2007], and no more than 50 such events have been detected for more than

five years. It was, however, recorded during the day, whereas the ERG (Arase) satellite observed all cases of hectometric continuum at night and in the morning. Kuril'chik [2007] also suggests that the hectometric radiation occurs near solar minimum. A similar assumption about the influence of solar activity on the generation of hectometric continuum radiation has been made in [Hashimoto et al., 2021], where generation of this radiation is associated with equatorial plasma bubbles since during solar minimum the rate of occurrence of bubbles after midnight increases at the summer solstice [Dao et al., 2011; Otsuka, 2018].

The characteristics of the hectometric radiation in Earth's magnetosphere, as well as, for comparison, similar characteristics of the kilometric continuum and AKR we have obtained in this work are presented in Table.

The main findings of this study are as follows:

- We have carried out a statistical analysis of cases of hectometric continuum radiation observation for a type A source(s) for a two-year period (279 cases).
- The relationship between hectometric continuum generation and local magnetic time has been confirmed. Radiation of this type is observed at night and in the morning.
- We have established that there is no direct relationship between the occurrence of hectometric radiation and geomagnetic disturbances.

The hectometric continuum radiation source(s) is located at low latitudes.

Characteristics of AKR, non-thermal and hectometric continuums

Parameters	Auroral kilometric radiation	Non-thermal continuum radiation	Hectometric continuum radiation
Frequency range	30–800 kHz	5–800 kHz	600–1700 kHz
Dependence on geomagnetic activity	high	present	absent
Radiation source localization	high latitudes	equatorial latitudes	low latitudes
Generation mechanism	Cyclotron maser instability	Linear or nonlinear mode conversion	currently unknown
Time of recording (MLT)	at night	mostly during the day	at night and in the morning

We express our gratitude to A. Kumamoto, Y. Kasahara, F. Tsuchiya for providing data from the PWE/HFA instrument of the ERG (Arase) satellite, which we have used in this work. The ERG (Arase) satellite data, as well as the description and characteristics of scientific instruments were taken from the ERG Research Center, led by ISAS/JAXA and ISEE/Nagoya University, on the website [<https://ergsc.isee.nagoya-u.ac.jp/>] [Miyoshi et al., 2018a, b]. The study analyzes PWE HFA-L2 v01.01. data [Kasahara et al., 2018; Kumamoto et al., 2018]. We are also grateful to the team of the World Data Center for Geomagnetism, Kyoto [<https://wdc.kugi.kyoto-u.ac.jp/>] for providing data on the *Dst* index. The work of A.A. Chernyshov was supported by the Foundation for the Development of Theoretical Physics and Mathematics “BASIS”.

REFERENCES

- Benediktov E.A., Getmancev G.G., Mitjakov N.A., Rapoport V.A., Sazonov Ju.A., Tarasov A.F. Results of measuring the intensity of radio emissions at 725 and 1525 kHz frequencies using the equipment installed on “ELECTRON-2” satellite. *Issledovaniya kosmicheskogo prostranstva* [Space exploration]. Moscow, Nauka Publ., 1965, 581 p. (In Russian).
- Benson R.F., Calvert W. ISIS-1 observations of the source of AKR. *Geophys. Res. Lett.* 1979, vol. 6, p. 479.
- Brown L.W. The galactic radio spectrum between 130 kHz and 2600 kHz. *Astrophys. J.* 1973, vol. 180, pp. 359–370.
- Carpenter D.L., Anderson R.R., Calvert W., Moldwin M.B. CRRES Observations of Density Cavities Inside the Plasmasphere. *J. Geophys. Res.* 2000, vol. 105, pp. 23323–23338. DOI: [10.1029/2000JA000013](https://doi.org/10.1029/2000JA000013).
- Chernyshov A.A., Chugunin D.V., Mogilevsky M.M. Auroral kilometric radiation as a diagnostic tool for the properties of the magnetosphere. *JETP Lett.* 2022, vol. 115, iss. 1, pp. 23–28. DOI: [10.1134/S0021364022010076](https://doi.org/10.1134/S0021364022010076).

- Chugunin D.V., Chernyshov A.A., Moiseenko I.L., Viktorov M.E., Mogilevsky M.M. Monitoring of the electron-acceleration region with auroral kilometric radiation. *Geomagnetism and Aeronomy*. 2020, vol. 60, iss. 5, pp. 538–546. DOI: [10.1134/S0016793220040039](https://doi.org/10.1134/S0016793220040039).
- Dao E., Kelley M.C., Roddy P., Retterer J.M., Ballenthin J., de La Beaujardiere O., Su Y.-J. Longitudinal and seasonal dependence of nighttime equatorial plasma density irregularities during solar minimum detected on the C/NOFS satellite. *Geophys. Res. Lett.* 2011, vol. 38, iss. 1, L10104. DOI: [10.1029/2011GL047046](https://doi.org/10.1029/2011GL047046).
- Green J.L., Sandel B.R., Fung S.F., Gallagher D.L. Reinisch B. On the origin of kilometric continuum. *J. Geophys. Res.* 2002, vol. 107, no. A7, 1105. DOI: [10.1029/2001JA000193](https://doi.org/10.1029/2001JA000193).
- Green J.L., Boardsen S., Fung S.F., Matsumoto H., Hashimoto K., Anderson R.R., et al. Association of kilometric continuum radiation with plasmaspheric structures. *J. Geophys. Res.* 2004, vol. 109, A03203. DOI: [10.1029/2003JA010093](https://doi.org/10.1029/2003JA010093).
- Gurnett D.A. The Earths as a radio source: Terrestrial kilometric radiation. *J. Geophys. Res.* 1974, vol. 79, iss. 28, pp. 4227–4238. DOI: [10.1029/JA079I028P04227](https://doi.org/10.1029/JA079I028P04227).
- Gurnett D.A. The Earth as a radio source: The nonthermal continuum. *J. Geophys. Res.* 1975, vol. 80, pp. 2751–2763. DOI: [10.1029/JA080I019P02751](https://doi.org/10.1029/JA080I019P02751).
- Hanasz J., de Feraudy H., Schreiber R., Parks G., Brittnacher M., Mogilevsky M.M., Romantsova T.V. Wide-band bursts of auroral kilometric radiation and their association with UV auroral bulges. *J. Geophys. Res.* 2001, vol. 106, pp. 3859–3872. DOI: [10.1029/2000JA900098](https://doi.org/10.1029/2000JA900098).
- Hashimoto K., Calvert K.W., Matsumoto H. Kilometric continuum detected by GEOTAIL. *J. Geophys. Res.* 1999, vol. 104, pp. 28645–28656. DOI: [10.1029/1999JA900365](https://doi.org/10.1029/1999JA900365).
- Hashimoto K., Anderson R.R., Green J.L., Matsumoto H. Source and propagation characteristics of kilometric continuum observed with multiple satellites. *J. Geophys. Res.* 2005, vol. 110, A09229. DOI: [10.1029/2004JA010729](https://doi.org/10.1029/2004JA010729).
- Hashimoto K., Kumamoto A., Tsuchiya F., Kasahara Y., Matsuoka A. Hectometric line spectra detected by the Arase (ERG) satellite. *Geophys. Res. Lett.* 2018, vol. 45, iss. 21, pp. 11555–11561. DOI: [10.1029/2018GL080133](https://doi.org/10.1029/2018GL080133).
- Hashimoto K., Shinbori A., Otsuka Y., Tsuchiya F., Kumamoto A., Kasahara Y., et al. Propagation mechanism of medium wave broadcasting waves observed by the Arase satellite: Hectometric line spectra. *J. Geophys. Res.* 2021, vol. 126, iss. 11, e2021JA029813. DOI: [10.1029/2021JA029813](https://doi.org/10.1029/2021JA029813).
- Jones D. Latitudinal beaming of planetary radio emissions. *Nature*. 1980, vol. 288, pp. 225–229. DOI: [10.1038/288225A0](https://doi.org/10.1038/288225A0).
- Kasaba Y., Matsumoto H., Hashimoto K., Anderson R.R. The angular distribution of auroral kilometric radiation observed by GEOTAIL spacecraft. *Geophys. Res. Lett.* 1997, vol. 24, pp. 2483–2486.
- Kasaba Y., Matsumoto H., Hashimoto K., Anderson R.R., Bougeret J.-L., Kaiser M.L., et al. Remote sensing of the plasma-pause during substorms: GEOTAIL observation of nonthermal continuum enhancement. *J. Geophys. Res.: Atmos.* 1998, vol. 103, no. A9, pp. 20389–20406. DOI: [10.1029/98JA00809](https://doi.org/10.1029/98JA00809).
- Kasahara Y., Kasaba Y., Kojima H., et al. The Plasma Wave Experiment (PWE) on board the Erase (ERG) satellite. *Earth, Planets and Space*. 2018, vol. 70, 86. DOI: [10.1186/s40623-018-0842-4](https://doi.org/10.1186/s40623-018-0842-4).
- Kolpak V.I., Mogilevsky M.M., Chugunin D.V., Chernyshov A.A., Moiseenko I.L., Kumamoto A., et al. Statistical properties of auroral kilometer radiation: based on ERG (Arase) satellite data. *Solar-Terr. Phys.* 2021, vol. 7, no. 1, pp. 11–16. DOI: [10.12737/stp-71202102](https://doi.org/10.12737/stp-71202102).
- Kumamoto A., Tsuchiya F., Kasahara Y., Kasaba Y., Kojima H., Yagitani S., et al. High Frequency Analyzer (HFA) of Plasma Wave Experiment (PWE) onboard the Arase spacecraft. *Earth, Planets and Space*. 2018, vol. 70, 82. DOI: [10.1186/s40623-018-0854-0](https://doi.org/10.1186/s40623-018-0854-0).
- Kuril'chik V.N. Observations of the auroral hectometric radio emissions onboard the INTERBALL-1 satellite. *Cosmic Res.* 2007, vol. 45, no. 3, pp. 248–252.
- Kuril'chik V.N., Grigor'eva V.P., Tirpak A., Mironov S.V., Fisher L., Yaroshevich A. Observations of a nonthermal continuum in the southern subpolar region of the Earth's magnetosphere by the Prognoz-10 INTERKOSMOS satellite. *Kosmicheskie issledovaniya [Cosmic Research]*. 1992, vol. 30, no. 2, pp. 231–242. (In Russian).
- Kuril'chik V.N., Kopaeva I.F., Mironov S.V. INTERBALL-1 observations of the kilometric “continuum” of the Earth's magnetosphere. *Cosmic Res.* 2004, vol. 42, no. 1, pp. 1–7.
- Kurth W.S. Detailed observations of the source of terrestrial narrowband electromagnetic radiation. *Geophys. Res. Lett.* 1982, vol. 9, pp. 1341–1344.
- Kurth W.S., Murata T., Lu G., Gurnett D.A., Matsumoto H. Auroral kilometric radiation and the auroral electrojet index for the January 1997 magnetic cloud event. *Geophys. Res. Lett.* 1998, vol. 25, iss. 15, pp. 3027–3030. DOI: [10.1029/98GL00404](https://doi.org/10.1029/98GL00404).
- Louarn P., Le Quéau D. Generation of the auroral kilometric radiation in plasma cavities — II. The cyclotron maser instability in small size sources. *Planet. Space Sci.* 1996, vol. 44, no. 3, pp. 211–224.
- Melrose D.B. A theory for the nonthermal radio continua in the terrestrial and Jovian magnetospheres. *J. Geophys. Res.* 1981, vol. 86, pp. 30–36. DOI: [10.1029/JA086IA01P00030](https://doi.org/10.1029/JA086IA01P00030).
- Miyoshi Y., Shinohara I., Takashima T., Asamura K., Higashio N., Mitani T., et al. Geospace exploration project ERG. *Earth, Planets and Space*. 2018a, vol. 70, 101. DOI: [10.1186/s40623-018-0862-0](https://doi.org/10.1186/s40623-018-0862-0).
- Miyoshi Y., Hori T., Shoji M., Teramoto M., Chang T.F., Segawa T., et al. The ERG Science Center. *Earth, Planets and Space*. 2018b, vol. 70, 96. DOI: [10.1186/s40623-018-0867-8](https://doi.org/10.1186/s40623-018-0867-8).
- Mogilevsky M.M., Moiseenko I.L., Hanasz J. Spectral variations and long-period intensity variations of auroral kilometric radiation from INTERBALL-2 satellite measurements. *Astron. Lett.* 2005, vol. 31, no. 6, pp. 422–426.
- Mogilevsky M.M., Chugunin D.V., Chernyshov A.A., Romantsova T.V., Moiseenko I.L., Kumamoto A., et al. Localization of sources of two types of continuum radiation. *JETP Lett.* 2021, vol. 114, pp. 23–28. DOI: [10.1134/S0021364021130075](https://doi.org/10.1134/S0021364021130075).
- Morooka M., Mukai T. Density as a controlling factor for seasonal and latitudinal variations of the auroral particle acceleration region. *J. Geophys. Res.* 2003, vol. 108, no. A7, 1306. DOI: [10.1029/2002JA009786](https://doi.org/10.1029/2002JA009786).
- Okuda H., Chance M.S., Ashour-Abdalla M., Kurth W.S. Generation of nonthermal continuum radiation in the magnetosphere. *J. Geophys. Res.* 1982, vol. 87, no. A12, pp. 10457–10462.
- Otsuka Y. Review of the generation mechanisms of post-midnight irregularities in the equatorial and low-latitude ionosphere. *Progress Earth Planet. Sci.* 2018, vol. 5, iss. 1, 57. DOI: [10.1186/s40645-018-0212-7](https://doi.org/10.1186/s40645-018-0212-7).
- Ronnmark K. Generation of magnetospheric radiation by decay of Bernstein waves. *Geophys. Res. Lett.* 1985, vol. 12, pp. 639–642. DOI: [10.1029/GL012i010p00639](https://doi.org/10.1029/GL012i010p00639).
- Treumann R.A. The electron-cyclotron maser for astrophysical application. *Astron. Astrophys. Rev.* 2006, vol. 13, no. 4, pp. 229–315. DOI: [10.1007/s00159-006-0001-y](https://doi.org/10.1007/s00159-006-0001-y).
- Turner J., Zarka P., Grießmeier J.-M., Lazio J., Cecconi B., Enriquez J.E., et al. The search for radio emissions from

the exoplanetary systems 55 Cancri, υ Andromedae, and τ Boötis using LOFAR beam-formed observations. *Astron. Astrophys.* 2021, vol. 645, A59, 28 p. DOI: [10.1051/0004-6361/201937201](https://doi.org/10.1051/0004-6361/201937201).

Voots G.R., Gurnett D.A., Akasofu S.I. Auroral kilometric radiation as an indicator of auroral magnetic disturbances. *J. Geophys. Res.* 1977, vol. 82, iss. 16, p. 2259.

Wu C.S., Lee L.C. A theory of the terrestrial kilometric radiation *Astrophys. J.* 1979, vol. 230, p. 621. DOI: [10.1086/157120](https://doi.org/10.1086/157120).

Zarka P. Auroral radio emissions at the outer planets: Observations and theories. *J. Geophys. Res.* 1998, vol. 103, pp. 20159–20194. DOI: [10.1029/98JE01323](https://doi.org/10.1029/98JE01323).

Zheleznyakov V.V., Zlotnik E.Ya., Zaitsev V.V., Shaposhnikov V.E. Double plasma resonance and its manifestations in radio astronomy. *Phys. Usp.* 2016, vol. 59, iss. 10, pp. 997–1020. DOI: [10.3367/UFNe.2016.05.037813](https://doi.org/10.3367/UFNe.2016.05.037813).

World Data Center for Geomagnetism, Kyoto; Nose M., Iyemori T., Sugiura M., Kamei T. *Geomagnetic Dst index*. 2015. DOI: [10.17593/14515-74000](https://doi.org/10.17593/14515-74000).

URL: <https://ergsc.isee.nagoya-u.ac.jp/> (accessed July 5, 2023).

URL: <https://wdc.kugi.kyoto-u.ac.jp/> (accessed July 5, 2023).

Original Russian version: Dorofeev D.A., Chernyshov A.A., Chugunin D.V., Mogilevsky M.M., published in *Solnechno-zemnaya fizika*. 2023. Vol. 9. Iss. 4. P. 71–79. DOI: [10.12737/szf-94202308](https://doi.org/10.12737/szf-94202308). © 2023 INFRA-M Academic Publishing House (Nauchno-Izdatelskii Tsentr INFRA-M)

How to cite this article

Dorofeev D.A., Chernyshov A.A., Chugunin D.V., Mogilevsky M.M. Main statistical properties of hectometric continuum radiation in near-Earth space. *Solar-Terrestrial Physics*. 2023. Vol. 9. Iss. 4. P. 63–71. DOI: [10.12737/stp-94202308](https://doi.org/10.12737/stp-94202308).